IEEE Access
Multidisciplinary : Rapid Review : Open Access Journal

Received 14 January 2023, accepted 7 February 2023, date of publication 14 February 2023, date of current version 23 February 2023.

Digital Object Identifier 10.1109/ACCESS.2023.3244830

RESEARCH ARTICLE

Introducing Improved Iterated Extended Kalman Filter (IIEKF) to Estimate the Rotor Rotational Speed, Rotor and Stator Resistances of Induction Motors

BIJAN MOAVENI [1], **ZAHRA MASOUMI** [2], **AND PEGAH RAHMANI** [2]
[1]Faculty of Electrical Engineering, Centre of Excellence for Modelling and Control of Complex Systems, K. N. Toosi University of Technology, Tehran 19967-15433, Iran
[2]School of Railway Engineering, Iran University of Science and Technology, Tehran 13114-16846, Iran

Corresponding author: Zahra Masoumi (z_masoumi@rail.iust.ac.ir)

ABSTRACT This paper introduces the Improved Iterated Extended Kalman Filter (IIEKF) for estimating the rotational speed, rotor resistance, and stator resistance of three-phase induction motors (IMs). Two state-space models for estimating the variables are presented. An optimal estimation of rotational speed is obtained by introducing a data fusion approach. The effectiveness of the IIEKF in comparison with the Extended Kalman Filter (EKF), using experimental data and in a wide range of operating conditions, is shown.

INDEX TERMS Induction motor, rotational speed, rotor and stator resistances, parameter estimation, extended Kalman filter.

I. INTRODUCTION

The induction motor (IM) parameters may change due to the winding temperature fluctuations, flux saturation, and skin effect [1]. Temperature variation can affect the rotor and stator resistances, while it has no remarkable effect on inductances. Conversely, high current values cause saturation of inductances [2].

Many control strategies of IMs, like Field Oriented Control (FOC), require accurate values of IM parameters, therefore, several methodologies have been presented to estimate the IM parameters [3], [4]. In recent years, sensorless estimation of rotational speed and rotor flux has attracted considerable attention in the introduced control strategies [5], [6]. In addition to the control strategies, the estimation of IM parameters is one of the conventional methods for fault detection [7], [8], [9], [10].

Generally, there are a large number of studies on estimating IM parameters. These studies can be categorized into three main groups: (i) model reference adaptive system methods, (ii) observer-based methods, and (iii) artificial intelligence techniques [11], [12], [13], [14], [15].

In [16], an artificial neural network has been designed to speed estimated through the estimation of stator current with the purpose of direct torque control of three-phase IM. It is worth noting that such data-driven methods require a considerable volume of data at different operating conditions of the motor. This volume of data not only requires strong processors but also analyzing this data is a time-consuming process.

In [11], a Model Reference Adaptive System (MRAS) for online rotor time constant estimation has been introduced. In [17], a comprehensive review of speed estimation based on MRAS techniques has been conducted. This study showed that MRAS technique has not appropriate accuracy in the presence of measurement noise and uncertainties.

A wide range of literature has been published regarding parameter estimation of IMs based on observers [18], [19], [20], [21], [22], [23], [24], [25], [26]. Among methods in this category, the Kalman Filters (KFs) family uses information on both dynamical and statistical model parameters of IM to estimate optimal values [27]. Hence, unlike deterministic

The associate editor coordinating the review of this manuscript and approving it for publication was R. K. Saket.

TABLE 1. A brief review of various parameter estimation methods using the KF family.

Method	No. ref	Year	Applications	Achievements
KF	[28]	1998	Speed estimation	Speed estimation by using estimation of rotor flux by employing second-order KF
EKF	[29]	2002	Speed estimation of an IM drives	Achieving good performance of an EKF by presenting a real-coded genetic algorithm (GA) to optimize the noise covariance and weight matrices of the EKF, and ensuring filter stability and accuracy in speed estimation
	[30]	2017	Speed sensorless control of IM	Speed estimation by suggesting an optimal EKF using an algorithm based on differential evolution to select accurate covariance matrices
	[25]	2020	Estimation of the stator stationary axis components of stator currents, rotor fluxes, rotor angular speed, and load torque	Improving estimation performance by increasing the order of EKF (developed six order EKF to eight order EKF) by using the data of speed sensor
Braided EKF	[31]	2008	Sensorless control of IM under speed and load variations, considering noise measurements	Increasing the accuracy in the estimation of rotor and stator resistances in comparison with single EKF
Adaptive EKF	[32], [23]	2018, 2020	Estimation of the stator stationary axis components of stator currents, the stator stationary axis components of rotor fluxes, the rotor mechanical speed, and the load torque for speed sensorless control	Presenting an innovation-based adaptive estimation approach to determine the covariance matrices, which results in better performance in comparison with EKF
	[33]	2021	Sensorless control of IM	Determining covariance matrices in EKF based on the maximum likelihood estimation criterion with limited memory exponential weighting
Hybrid Adaptive EKF	[26]	2022	State Estimation of IM for speed sensorless control, fault-tolerant control, and fault diagnosis	Improving the estimation quality of adaptive EKF by combining the advantages of innovation-based EKFs and adaptive fading-based EKFs
UKF	[43]	2006	Estimated of rotor speed and dq-axis fluxes of an IM	Presenting UKF and showing that the intrinsic properties of UKF are more satisfactory than EKF in highly nonlinear systems using the same covariance matrices in both EKF and UKF approaches
	[44]	2020	Estimation of the stator stationary axis components of stator currents, the stator stationary axis components of rotor fluxes, the rotor mechanical speed, and the load torque	Presenting the comparison of EKF and UKF approaches that both methods have similar estimation performances when the same covariance matrices are used. Both methods are affected by variations of mutual inductance, stator, and rotor resistances.

observers, the stochastic nature of the KF addresses the issues regarding the model uncertainties and measurement noise of IM [23].

In recent studies on the estimation and identification of IM parameters using KF and its extensions, speed estimation of IM for employing speed sensorless control has been considerable [23], [28], [29], [30], [31], [32], [33]. Table 1 presents a brief review of some studies of various types of KFs used to estimate IM parameters. According to Table 1, Extended KF (EKF) and Unscented KF (UKF) are two successful methods in the sensorless control strategy.

In [28], adaptive observers along with second-order KF were suggested to estimate flux and rotational speed. In [29], [34], and [35], the flux and speed were estimated using EKF. In [31], a braided EKF has been applied for sensorless control of IM under speed and load variations in the presence of measurement noise. Although EKF is employed for nonlinear processes, it basically uses a linearization approach to determine the current and covariance of the state [19]. Despite the wide use of this application, it has an obvious disadvantage in the case of filter instability due to the linearization, when sample time is not proper, affecting the Jacobian matrix and estimation results [19], [31]. It should be noted that in [29], [34], [35], [36], and [37], the speed is assumed as a constant parameter, affecting the estimation of transient speed. None of these studies estimate rotor resistance, changing during operation conditions, thereby affecting the estimation of parameters. However, in the case of [16] and [36] the effects of rotor resistance variation have been reflected. In [38], a single EKF using two extended IM models has been introduced as a BI-EKF algorithm to estimate load torque, rotor, and stator resistances.

In some studies about the controller design of IM, the estimation of rotor resistance has been considered [39], [41], [42]. In [39], using the direct FOC scheme, besides rotor flux and speed, rotor resistance was estimated using EKF. In [40] and [41], the authors estimated rotor resistance, speed, and rotor flux using the DTC scheme. In [42], a modified EKF has been used to decrease execution time for estimating the parameters of six-phase IM controlled by DTC.

This paper introduces an Improved Iterared EKF (IIEKF) to estimate rotor rotational speed, rotor, and stator resistances based on two extracted state-space models. Due to the nonlinear behavior of IM, IIEKF as a modified version of EKF has been introduced. The performance of IIEKF is studied under various machine operating conditions and load variations in a wide range of the rotational speed of IM. Also, the experimental results of employing IIEKF have been compared with the estimation results of EKF.

The organization of this paper is as follows: Section II presents the mathematical model of IM. After reviewing EKF and Iterated EKF (IEKF), IIEKF is introduced in section III. Section IV introduces the estimation method to estimate the rotational speed, rotor, and stator resistances of IM. In section V, the experimental results and discussion are presented. The conclusion is presented in section VI.

II. MATHEMATICAL MODEL OF INDUCTION MOTOR

The discrete-time dynamic equations of three-phase IM in a stationary frame, based on the stator currents and rotor fluxes can be written as [22]:

$$i_{ds}(k) = \left(-\frac{T_s}{\sigma L_s}R_s - \frac{L_m^2 T_s}{\sigma L_s L_r^2}R_r + 1\right) i_{ds}(k-1)$$

$$
\begin{aligned}
&+\left(\frac{L_m T_s}{\sigma L_s L_r^2} R_r\right) \lambda'_{dr}(k-1)+\frac{T_s}{\sigma L_s} v_{ds}(k-1)\\
&+\left(\frac{L_m T_s}{\sigma L_s L_r} n_p\right) \omega_r(k-1) \lambda'_{qr}(k-1) \qquad (1a)\\
i_{qs}(k) &=\left(-\frac{T_s}{\sigma L_s} R_s-\frac{L_m^2 T_s}{\sigma L_s L_r^2} R_r+1\right) i_{qs}(k-1)\\
&+\left(\frac{L_m T_s}{\sigma L_s L_r^2} R_r\right) \lambda'_{qr}(k-1)+\frac{T_s}{\sigma L_s} v_{qs}(k-1)\\
&-\left(\frac{L_m T_s}{\sigma L_s L_r} n_p\right) \omega_r(k-1) \lambda'_{dr}(k-1) \qquad (1b)\\
\lambda'_{dr}(k) &=\frac{L_m T_s}{L_r} R_r i_{ds}(k-1)-n_p T_s \omega_r(k-1) \lambda'_{qr}(k-1)\\
&+\left(-\frac{T_s}{L_r} R_r+1\right) \lambda'_{dr}(k-1) \qquad (1c)\\
\lambda'_{qr}(k) &=\frac{L_m T_s}{L_r} R_r i_{qs}(k-1)+n_p T_s \omega_r(k-1) \lambda'_{dr}(k-1)\\
&+\left(-\frac{T_s}{L_r} R_r+1\right) \lambda'_{qr}(k-1) \qquad (1d)\\
\omega_r(k) &=n_p \omega_r(k-1)-\frac{T_l}{J}\\
&+\frac{3 n_p L_m T_s}{2 J L_r}\left(i_{ds}(k-1) \lambda'_{qr}(k-1)\right.\\
&\left.-i_{qs}(k-1) \lambda'_{dr}(k-1)\right) \qquad (1e)
\end{aligned}
$$

where, $i_{ds}(k)$ and $i_{qs}(k)$ are the stator current elements, $v_{ds}(k)$ and $v_{qs}(k)$ are the stator voltage elements, $\lambda'_{dr}(k)$ and $\lambda'_{qr}(k)$ are rotor flux linkage elements in dq reference frame. $\omega_r(k)$ is the rotor rotational speed. L_m, L_r, and L_s are the mutual inductance, rotor and stator self-inductances, respectively. R_r and R_s are the rotor and stator resistances, respectively. n_p is the number of poles of IM. J is the total inertia of the IM, T_l is the load torque and σ is the total leakage coefficient that it can be defined as follows [45]:

$$\sigma=1-\left(\frac{L_m^2}{L_r L_s}\right) \qquad (2)$$

III. IMPROVED ITERATED EXTENDED KALMAN FILTER

EKF is an extension of KF for nonlinear dynamics systems. EKF approximates the nonlinearities using linearization around the last estimated value of the state variables. The general framework for EKF was introduced in [46]. IEKF and UKF, as modified versions of EKF, are two alternative filters for linearization first-order approximation errors of the EKF [47]. The estimation performances of UKF and EKF are similar by using the same covariance matrices [44] and greatly degraded in the presence of observation outliers due to their lack of robustness [48], similar to [49] employing a version of IEKF (IIEKF) has been suggested in this study. Although IEKF requires relatively more computational time compared to EKF, implementation of this filter results in the desired estimation by decreasing estimation error [49]. IEKF equations are presented as follows.

Consider the nonlinear state-space model of a system in the discrete-time domain as (3).

$$
\begin{aligned}
\mathbf{x}(k) &=\mathbf{f}(\mathbf{x}(k-1), \mathbf{u}(k-1))+\mathbf{w}(k-1) \qquad (3a)\\
\mathbf{z}(k) &=\mathbf{h}(\mathbf{x}(k))+\mathbf{v}(k) \qquad (3b)
\end{aligned}
$$

In these equations, $\mathbf{w}(k)$ and $\mathbf{v}(k)$ are denoted as process noise and measurement noise with covariance matrix $\mathbf{Q}(k)$ and $\mathbf{R}(k)$, respectively. $\mathbf{f}(.)$ and $\mathbf{h}(.)$ are nonlinear continuous functions. To linearize nonlinear functions, $\mathbf{f}(.)$ and $\mathbf{h}(.)$, equations (4) to (6) are represented as follows, where $\mathbf{F}(.)$, $\Gamma(.)$ and $\mathbf{H}(.)$ are the Jacobian matrices.

$$
\begin{aligned}
\mathbf{F}(\hat{\mathbf{x}}(k-1), \mathbf{u}(k-1)) &=\left.\frac{\partial \mathbf{f}}{\partial \mathbf{x}}\right|_{(\hat{\mathbf{x}}(k-1), \mathbf{u}(k-1))} \qquad (4)\\
\Gamma(\hat{\mathbf{x}}(k-1), \mathbf{u}(k-1)) &=\left.\frac{\partial \mathbf{f}}{\partial \mathbf{u}}\right|_{(\hat{\mathbf{x}}(k-1), \mathbf{u}(k-1))} \qquad (5)\\
\mathbf{H}(\hat{\mathbf{x}}^{-}(k)) &=\left.\frac{\partial \mathbf{h}}{\partial \mathbf{x}}\right|_{\hat{\mathbf{x}}^{-}(k)} \qquad (6)
\end{aligned}
$$

Generally, by determining the initial values as (7), IEKF equations are presented as (8), which can be separated into two parts (measurement update and time update).

$$
\begin{aligned}
\hat{\mathbf{x}}^{-}(0) &=E[\mathbf{x}(0)] \qquad (7a)\\
\mathbf{P}^{-}(0) &=E\left[\left(\mathbf{x}(0) \hat{\mathbf{x}}^{-}(0)\right)\left(\mathbf{x}(0) \hat{\mathbf{x}}^{-}(0)\right)^T\right] \qquad (7b)
\end{aligned}
$$

Measurement update:

$$
\begin{aligned}
\hat{\mathbf{x}}^{+}(k, 0) &=\hat{\mathbf{x}}^{-}(k) \qquad (8a)\\
\mathbf{P}^{+}(k, 0) &=\mathbf{P}^{-}(k) \qquad (8b)\\
\mathbf{K}(k) &=\mathbf{P}^{+}(k, i) \mathbf{H}^T(\hat{\mathbf{x}}^{+}(k, i))\\
&\times\left(\mathbf{H}(\hat{\mathbf{x}}^{+}(k, i)) \mathbf{P}^{+}(k, i) \mathbf{H}^T(\hat{\mathbf{x}}^{+}(k, i))\right.\\
&\left.+\mathbf{R}(k)\right)^{-1} \qquad (8c)\\
\hat{\mathbf{x}}^{+}(k, i+1) &=\hat{\mathbf{x}}^{+}(k, i)+\mathbf{K}(k)\left(\mathbf{z}(k)-\mathbf{h}\left(\mathbf{x}^{+}(k, i)\right)\right) \qquad (8d)\\
\mathbf{P}^{+}(k, i+1) &=\left(\mathbf{I}-\mathbf{K}(k) \mathbf{H}(\hat{\mathbf{x}}^{+}(k, i))\right) \mathbf{P}^{+}(k, i) \qquad (8e)\\
i &=N \qquad (8f)
\end{aligned}
$$

Time update:

$$
\begin{aligned}
\mathbf{P}(k) &=\mathbf{P}^{+}(k, N+1) \qquad (8g)\\
\hat{\mathbf{x}}(k) &=\hat{\mathbf{x}}^{-}(k, N+1) \qquad (8h)\\
\mathbf{P}^{-}(k+1) &=\mathbf{F}(\hat{\mathbf{x}}(k), \mathbf{u}(k)) \mathbf{P}(k) \mathbf{F}^T(\hat{\mathbf{x}}(k), \mathbf{u}(k))+\mathbf{Q}(k) \qquad (8i)\\
\hat{\mathbf{x}}^{-}(k+1) &=\mathbf{f}(\hat{\mathbf{x}}(k), \mathbf{u}(k)) \qquad (8j)
\end{aligned}
$$

where, $\mathbf{P}^{-}(k)$ and $\hat{\mathbf{x}}^{-}(k)$ are the a priori estimation of $\mathbf{P}(k)$ and $\hat{\mathbf{x}}(k)$ using $\mathbf{Z}^{-}=\{\mathbf{z}(1) \ldots \mathbf{z}(k-1)\}$, respectively. Since the linearized system may become unobservable in some operating points, it is suggested to check observability before the time update part. If the states are unobservable, the states do not update. In other words, in IIEKF, (8h) is substituted by (18).

$$
\begin{aligned}
\varphi=\Big[\, & \mathbf{H}^T(\hat{\mathbf{x}}^{-}(k)) \quad \left(\mathbf{H}(\hat{\mathbf{x}}^{-}(k)) \mathbf{F}(\hat{\mathbf{x}}(k-1), \mathbf{u}(k-1))\right)^T \ldots\\
& \left(\mathbf{H}(\hat{\mathbf{x}}^{-}(k)) \mathbf{F}^{n-1}(\hat{\mathbf{x}}(k-1), \mathbf{u}(k-1))\right)^T\Big]^T \qquad (9a)
\end{aligned}
$$

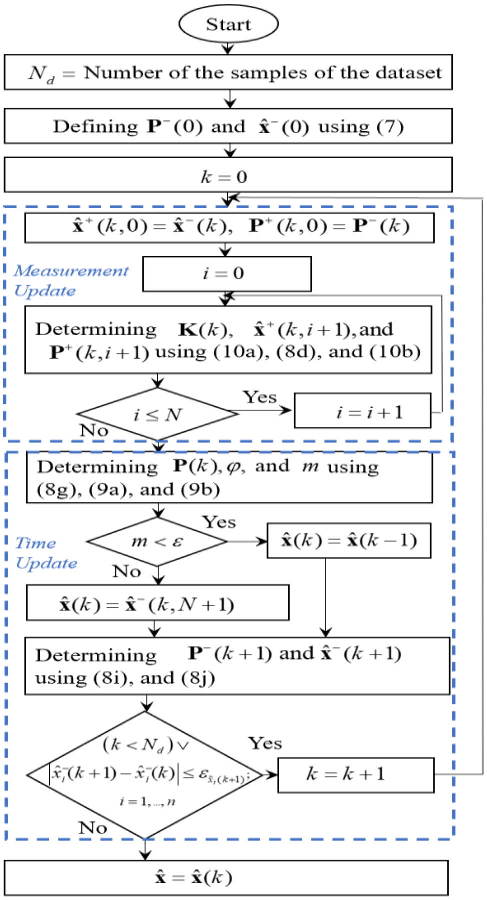

FIGURE 1. Flow chart of the introduced IIEKF.

$$\begin{cases} m_1 = \sigma_{\min}(\varphi) \\ m_2 = \sigma_{\max}(\varphi) \end{cases} \rightarrow m = \frac{m_1}{m_2} \tag{9b}$$

$$\begin{cases} m \ge \varepsilon \Rightarrow \hat{\mathbf{x}}(k) = \hat{\mathbf{x}}^-(k, N+1) \\ m < \varepsilon \Rightarrow \hat{\mathbf{x}}(k) = \hat{\mathbf{x}}(k-1) \end{cases} \tag{9c}$$

In (9), $\sigma_{\min}(\varphi)$ and $\sigma_{\max}(\varphi)$ are the minimum and maximum singular values of φ, respectively. ε, as a threshold, can be determined using (9b) when the system is completely observable. It is suggested that $\varepsilon = 10^{-5}$.

Besides, in the case of the covariance matrix $\mathbf{P}^+(k,i)$, implementing a forgetting factor, α which modifies the covariance matrix resulting in accurate and fast estimation. $\mathbf{P}^+(k,i)$ is substituted by $(1/\alpha)\mathbf{P}^+(k,i)$ in (8c) and (8e) that $0 < \alpha < 1$. In other words, (8c) and (8e) are substituted by (19).

$$\begin{aligned} \mathbf{K}(k) = {} & (1/\alpha)\,\mathbf{P}^+(k,i)\mathbf{H}^T(\hat{\mathbf{x}}^+(k,i)) \\ & \times \Big((1/\alpha)\,\mathbf{H}(\hat{\mathbf{x}}^+(k,i))\mathbf{P}^+(k,i)\mathbf{H}^T(\hat{\mathbf{x}}^+(k,i)) \\ & + \mathbf{R}(k)\Big)^{-1} \end{aligned} \tag{10a}$$

$$\mathbf{P}^+(k,i+1) = \big(\mathbf{I} - \mathbf{K}(k)\mathbf{H}(\hat{\mathbf{x}}^+(k,i))\big)\,(1/\alpha)\,\mathbf{P}^+(k,i) \tag{10b}$$

The flow chart of the introduced IIEKF is shown in Figure 1. In Figure 1, by defining $\hat{\mathbf{x}}^-(k) = \left[\hat{x}_i^-(k)\right]_{n\times 1}$, $\varepsilon_{\tilde{x}_i(k)}$; $i = 1, \ldots, n$ are determined using the convergence of states. $\varepsilon_{\tilde{x}_i(k)}$ is suggested that, if $\left|\hat{x}_i^-(k)\right| < 1$, then $\varepsilon_{\tilde{x}_i(k)} = 0.01\hat{x}_i^-(k)$; otherwise, $\varepsilon_{\tilde{x}_i(k)} = 0.01$.

IV. ESTIMATION OF $\omega_r(k)$, R_r, AND R_s

In order to estimate $\omega_r(k)$, R_r, and R_s using IIEKF a discrete-time state-space model should be presented to introduce the dynamic behavior of $\omega_r(k)$, R_r, and R_s.

A. STATE-SPACE MODEL FOR ESTIMATING R_r AND $\omega_r(k)$

In order to estimate $\omega_r(k)$ and R_r, the state vector, $\mathbf{x_r}(k)$, and input vector, $\mathbf{u}(k)$, are defined as (11).

$$\begin{aligned} \mathbf{x_r}(k) &= \left[x_{r_i}(k)\right]_{6\times 1} \\ &= \begin{bmatrix} i_{ds}(k) & i_{qs}(k) & \lambda'_{dr}(k) & \lambda'_{qr}(k) & \omega_r(k) & R_r \end{bmatrix}^T \end{aligned} \tag{11a}$$

$$\mathbf{u}(k) = [u_i(k)]_{2\times 1} = \begin{bmatrix} v_{ds}(k) & v_{qs}(k) \end{bmatrix}^T \tag{11b}$$

Therefore, the augmented discrete-time state-space model is expressed as follows:

$$\mathbf{x_r}(k) = \mathbf{f}_r(\mathbf{x}_r(k-1), \mathbf{u}(k-1)) \tag{12a}$$

$$\mathbf{y_r}(k) = \mathbf{h_r}(\mathbf{x}_r(k)) \tag{12b}$$

where,

$$\begin{aligned} &\mathbf{f}_r(\mathbf{x}_r(k-1), \mathbf{u}(k-1)) \\ &\quad = \left[f_{r_i}(\mathbf{x}_r(k-1), \mathbf{u}(k-1))\right]_{6\times 1} \end{aligned} \tag{13a}$$

$$\begin{aligned} &f_{r_1}(\mathbf{x}_r(k), \mathbf{u}(k)) \\ &\quad = \left(\frac{L_m T_s}{\sigma L_s L_r} n_p\right) x_{r_5}(k) x_{r_4}(k) \\ &\qquad + \left(-\frac{T_s}{\sigma L_s} R_s - \frac{L_m^2 T_s}{\sigma L_s L_r^2} x_{r_6}(k) + 1\right) x_{r_1}(k) \\ &\qquad + \left(\frac{L_m T_s}{\sigma L_s L_r^2} x_{r_6}(k)\right) x_{r_3}(k) + \frac{T_s}{\sigma L_s} u_1(k) \end{aligned} \tag{13b}$$

$$\begin{aligned} &f_{r_2}(\mathbf{x}_r(k), \mathbf{u}(k)) \\ &\quad = -\left(\frac{L_m T_s}{\sigma L_s L_r} n_p\right) x_{r_5}(k) x_{r_3}(k) \\ &\qquad + \left(-\frac{T_s}{\sigma L_s} R_s - \frac{L_m^2 T_s}{\sigma L_s L_r^2} x_{r_6}(k) + 1\right) x_{r_2}(k) \\ &\qquad + \left(\frac{L_m T_s}{\sigma L_s L_r^2} x_{r_6}(k)\right) x_{r_4}(k) + \frac{T_s}{\sigma L_s} u_2(k) \end{aligned} \tag{13c}$$

$$\begin{aligned} &f_{r_3}(\mathbf{x}_r(k), \mathbf{u}(k)) \\ &\quad = -n_p T_s x_{r_5}(k) x_{r_4}(k) \\ &\qquad + \frac{L_m T_s}{L_r} x_{r_6}(k) x_{r_1}(k) + \left(-\frac{T_s}{L_r} x_{r_6}(k) + 1\right) x_{r_3}(k) \end{aligned} \tag{13d}$$

$$\begin{aligned} &f_{r_4}(\mathbf{x}_r(k), \mathbf{u}(k)) \\ &\quad = -n_p T_s x_{r_5}(k) x_{r_3}(k) \\ &\qquad + \frac{L_m T_s}{L_r} x_{r_6}(k) x_{r_2}(k) + \left(-\frac{T_s}{L_r} x_{r_6}(k) + 1\right) x_{r_4}(k) \end{aligned} \tag{13e}$$

$$\begin{aligned} &f_{r_5}(\mathbf{x}_r(k), \mathbf{u}(k)) \\ &\quad = n_p x_{r_5}(k) \end{aligned}$$

$$-\frac{T_l}{J}+\frac{3n_pL_mT_s}{2JL_r}\left(x_{r_1}(k)x_{r_4}(k)-x_{r_2}(k)x_{r_3}(k)\right) \tag{13f}$$

$$f_{r_6}(\mathbf{x}_r(k-1) = x_{r_6}(k) \tag{13g}$$

$$\mathbf{h_r}(\mathbf{x}_r(k)) = \begin{bmatrix} x_{r_1}(k) & x_{r_2}(k) \end{bmatrix}^T \tag{14}$$

Consequently, $\mathbf{F_r}(\mathbf{x_r}(k-1), \mathbf{u}(k-1)), \Gamma_\mathbf{r}(\mathbf{x_r}(k-1), \mathbf{u}(k-1))$, and $\mathbf{H_r}(\mathbf{x_r}(k))$ as the Jacobian matrices in (4)-(7) are obtained as (15)-(17) for employing IIEKF.

$$\mathbf{F_r}(\mathbf{x}_r(k-1), \mathbf{u}(k-1)) = \mathbf{I}_{6\times6} + T_s\begin{bmatrix} -\left(\frac{R_s}{\sigma L_s}+\frac{x_{r_6}(k-1)L_m^2}{L_r^2\sigma L_s}\right)\mathbf{I}_{2\times2} & \mathbf{F_1} & \mathbf{0}_{2\times2} \\ x_{r_6}(k-1)\frac{L_m}{L_r}\mathbf{I}_{2\times2} & \mathbf{F}_2 & \mathbf{0}_{2\times2} \\ -\frac{3n_p}{2J_l}\frac{L_m}{L_r}x_{r_4}(k-1)\mathbf{I_1} & \mathbf{0}_{2\times2} & \mathbf{0}_{2\times2} \end{bmatrix} \tag{15}$$

$$\Gamma_\mathbf{r}(\mathbf{x_r}(k-1), \mathbf{u}(k-1)) = \begin{bmatrix} \frac{T}{L_\sigma}\mathbf{I}_{2\times2} & \mathbf{0}_{2\times4} \end{bmatrix}^T \tag{16}$$

$$\mathbf{H_r}(\mathbf{x_r}(k)) = \begin{bmatrix} \mathbf{I}_{2\times2} & \mathbf{0}_{2\times4} \end{bmatrix} \tag{17}$$

where,

$$\mathbf{I_1} = \begin{bmatrix} 1 & 1 \\ 0 & 0 \end{bmatrix} \tag{18a}$$

$$\mathbf{F_1} = \begin{bmatrix} \frac{R_rL_m}{L_r^2\sigma L_s} & \frac{L_mn_p\omega_m}{L_r\sigma L_s} \\ -\frac{L_mn_p\omega_m}{L_r\sigma L_s} & -\frac{R_rL_m}{L_r^2\sigma L_s} \end{bmatrix} \tag{18b}$$

$$\mathbf{F}_2 = \begin{bmatrix} -\frac{R_r}{L_r} & -n_p\omega_m \\ -n_p\omega_m & -\frac{R_r}{L_r} \end{bmatrix} \tag{18c}$$

B. STATE-SPACE MODEL FOR ESTIMATING R_s AND $\omega_r(k)$

In this case, to estimate R_s and $\omega_r(k)$, the state vector, $\mathbf{x_s}(k) = [x_{s_i}(k)]_{6\times1}$, is defined as (29).

$$\mathbf{x_s}(k) = \begin{bmatrix} i_{ds}(k) & i_{qs}(k) & \lambda'_{dr}(k) & \lambda'_{qr}(k) & \omega_r(k) & R_s \end{bmatrix}^T \tag{19}$$

Same as the previous subsection, (22)-(28), the space-state model is defined as follows:

$$\mathbf{x_s}(k) = \mathbf{f_s}(\mathbf{x_s}(k-1), \mathbf{u}(k-1)) \tag{20a}$$

$$\mathbf{y_s}(k) = \mathbf{h_s}(\mathbf{x_s}(k)) \tag{20b}$$

where,

$$\mathbf{f_s}(\mathbf{x_s}(k-1), \mathbf{u}(k-1)) = [f_{s_i}(\mathbf{x_s}(k-1), \mathbf{u}(k-1))]_{6\times1} = \mathbf{f_r}(\mathbf{x_r}(k-1), \mathbf{u}(k-1))\Big|_{\substack{x_{r_i}(k)=x_{s_i}(k);\ i=1,\ldots,5 \\ x_{r_6}(k)=R_r \\ R_s=x_{s_6}(k)}} \tag{21}$$

$$\mathbf{h_s}(\mathbf{x}_s(k)) = \begin{bmatrix} x_{s_1}(k) & x_{s_2}(k) \end{bmatrix}^T \tag{22}$$

Then, for employing IIEKF according to (4)-(6), $\mathbf{F_s}(\mathbf{x_s}(k-1), \mathbf{u}(k-1)), \Gamma_\mathbf{s}(\mathbf{x_s}(k-1), \mathbf{u}(k-1))$, and $\mathbf{H_s}(\mathbf{x}_s(k))$ as the Jacobian matrices are obtained as (23)-(25).

$$\mathbf{F_s}(\mathbf{x}_s(k-1), \mathbf{u}(k-1)) = \mathbf{I}_{6\times6} + T_s\begin{bmatrix} -\left(\frac{x_{s_6}(k-1)}{\sigma L_s}+\frac{R_rL_m^2}{L_r^2\sigma L_s}\right)\mathbf{I}_{2\times2} & \mathbf{F_1} & \mathbf{0}_{2\times2} \\ R_r\frac{L_m}{L_r}\mathbf{I}_{2\times2} & \mathbf{F}_2 & \mathbf{0}_{2\times2} \\ -\frac{3n_p}{2J_l}\frac{L_m}{L_r}x_{s_4}(k-1)\mathbf{I_1} & \mathbf{0}_{2\times2} & \mathbf{0}_{2\times2} \end{bmatrix} \tag{23}$$

$$\Gamma_s(\mathbf{x}_s(k-1), \mathbf{u}(k-1)) = \begin{bmatrix} \frac{T}{L_\sigma}\mathbf{I}_{2\times2} & \mathbf{0}_{2\times4} \end{bmatrix}^T \tag{24}$$

$$\mathbf{H}_s(\mathbf{x}_s(k)) = \begin{bmatrix} \mathbf{I}_{2\times2} & \mathbf{0}_{2\times4} \end{bmatrix} \tag{25}$$

It should be noted that in (15) and (23) the variations of R_r and R_s with time are assumed to be really too small which can be considered constant parameters.

By considering the state-space models of the IM for estimating $\omega_r(k)$, R_r, and R_s in (12) and (20), two IIEKFs, which are presented in section III, Figure 1, are used simultaneously to estimate the state variables. In the first IIEKF, R_r and $\omega_r(k)$ will be estimated, where $\mathbf{x}(k) = \mathbf{x_r}(k), \hat{\mathbf{x}}(k) = \hat{\mathbf{x}}_\mathbf{r}(k), \mathbf{f}(.) = \mathbf{f}_r(.)$, and $\mathbf{h}(.) = \mathbf{h_r}(.)$. Therefore, according to (11), the estimations of R_r and $\omega_r(k)$ are obtained as follows :

$$\hat{R}_r = \hat{\mathbf{x}}_{r_6}(k) \tag{26a}$$

$$\hat{\omega}_r(k) = \hat{\mathbf{x}}_{r_5}(k) \tag{26b}$$

In the second IIEKF, by defining $\mathbf{x}(k) = \mathbf{x_s}(k), \hat{\mathbf{x}}(k) = \hat{\mathbf{x}}_\mathbf{s}(k), \mathbf{f}(.) = \mathbf{f}_s(.)$, and $\mathbf{h}(.) = \mathbf{h}_s(.)$, R_s and $\omega_r(k)$ will be estimated as follows:

$$\hat{R}_s = \hat{\mathbf{x}}_{s_6}(k) \tag{27a}$$

$$\hat{\omega}_r(k) = \hat{\mathbf{x}}_{s_5}(k) \tag{27b}$$

Since $\omega_r(k)$ is the state variable in both (11) and (19) state vectors, this variable is estimated twice. To achieve optimal state estimation between (26b) and (27b), we can use the data fusion method as follows [50]:

$$\hat{\omega}_r(k) = \frac{\left(\left(p_{55_r}(k)\right)^{-1}\hat{\mathbf{x}}_{r_5}(k)+\left(p_{55_s}(k)\right)^{-1}\hat{\mathbf{x}}_{s_5}(k)\right)}{\left(p_{55_r}(k)\right)^{-1}+\left(p_{55_s}(k)\right)^{-1}} \tag{28}$$

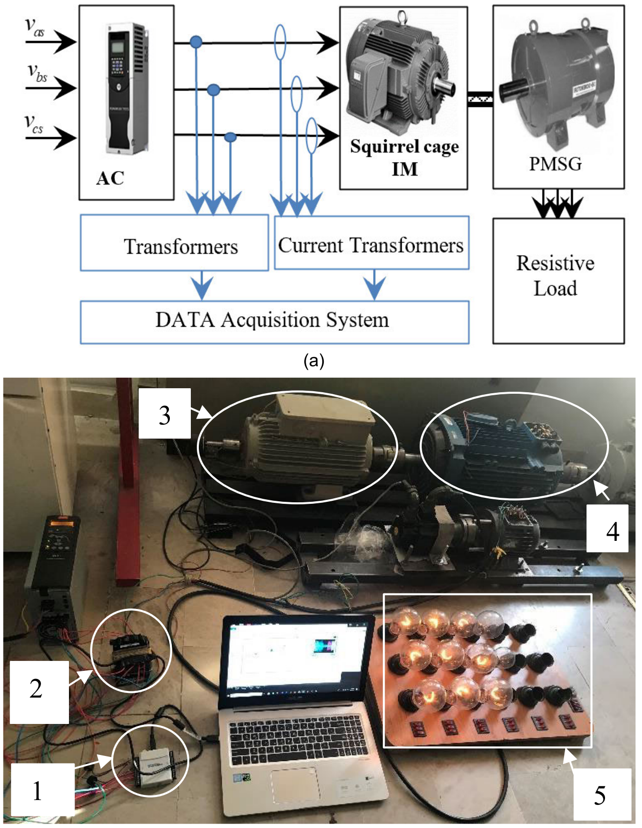

FIGURE 2. (a) A simplified block diagram of the experimental setup, (b) The experimental setup and data acquisition system, (1) NI USB6009, (2) Three-phase transformer (380/5) (3) Squirrel cage IM, (4) PMSG, (5) Resistive Loads.

In (28), $p_{55_r}(k)$ and $p_{55_s}(k)$ are the 5$^{\text{th}}$ diagonal element of $\mathbf{P}_r(k)$ and $\mathbf{P}_s(k)$, respectively. The mathematical definition of $\mathbf{P}_r(k)$ and $\mathbf{P}_s(k)$ are as follows:

$$\begin{cases} \mathbf{P}_r(k) = \left[p_{ij_r}(k)\right]_{6\times 6};\, i,j = 1,\ldots,6 \\ \qquad = \mathbf{P}(k)\text{in the } 1^{\text{st}}\text{IIEKF using to estimate } \mathbf{x_r}(k) \\ \mathbf{P}_s(k) = \left[p_{ij_s}(k)\right]_{6\times 6};\, i,j = 1,\ldots,6 \\ \qquad = \mathbf{P}(k)\text{in the } 2^{\text{st}}\text{IIEKF using to estimate}\mathbf{x}_s(k) \end{cases} \tag{29}$$

It should be noted that $\mathbf{P}_r(k)$ and $\mathbf{P}_s(k)$ are the error covariance matrices.

V. EXPERIMENTAL RESULTS AND DISCUSSION

In order to show the effectiveness of the introduced methodology to estimate $\omega_r(k)$, R_r, and R_s, the real input-output data of a 1.5 Kw squirrel cage IM were used. The technical specification of the IM has been given in Table 2. The experimental setup and data acquisition system are shown in Figure 2. The load of the IM was a permanent magnet synchronous generator (PMSG) and the load of the PMSG was the resistive load. The PMSG, as a mechanical load for IM, is used to change the load torque.

Two experiments were performed under different load torques in the nominal rotor rotational speed $\omega_r(k) = [0 \sim 3000](RPM)$, and lower than the nominal rotor rotational speed $\omega_r(k) = [0 \sim 1000](RPM)$. By considering stator voltages as inputs, (11), and stator currents as outputs variables, (12) and (20), stator voltages and currents are measured and recorded by NI USB6009. The stator voltages and

TABLE 2. Technical specifications of induction motor.

Parameter	Value	Parameter	Value
P_n	1.54 (KW)	R_r	4.53(Ω)
v_n	220(V)	R_s	5.63(Ω)
I_n	3(A)	L_r	489(mH)
ω_n	2820(RPM)	L_s	489(mH)
n_p	1	L_m	460(mH)
f_{sn}	50(Hz)	J	0.5 (kgm^2)

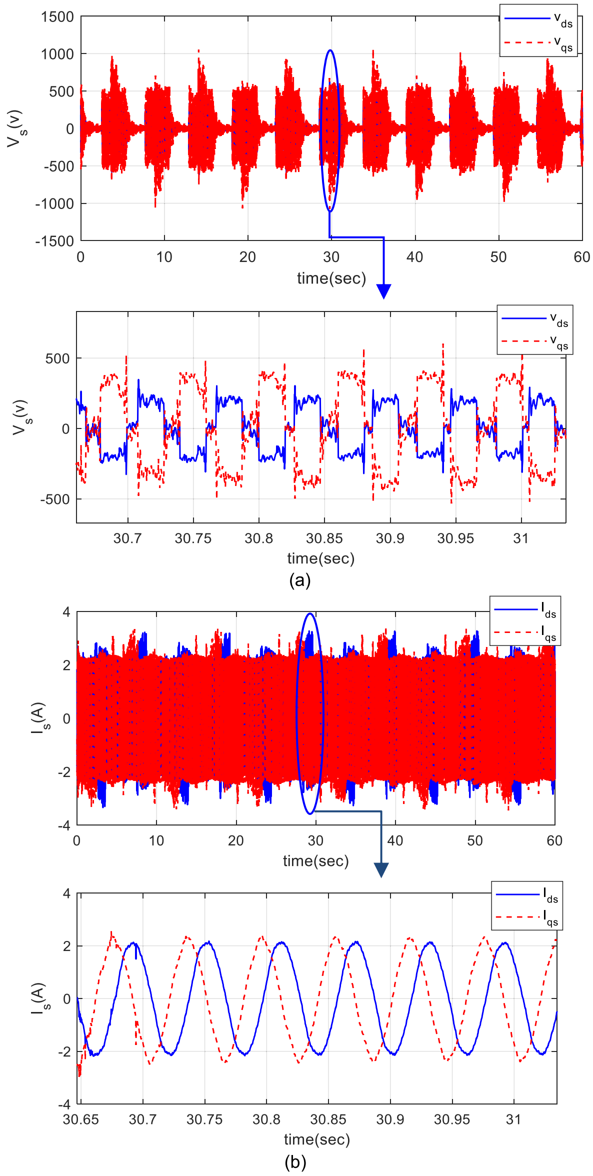

FIGURE 3. Stator elements in *dq* reference frame (a) stator voltage elements (b) stator current elements.

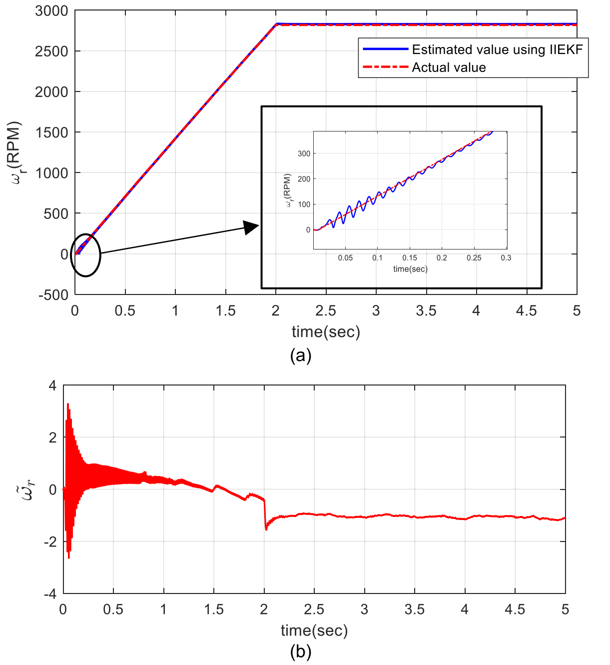

FIGURE 4. (a) Estimated of the rotor rotational speed and (b) Estimation error in nominal speed.

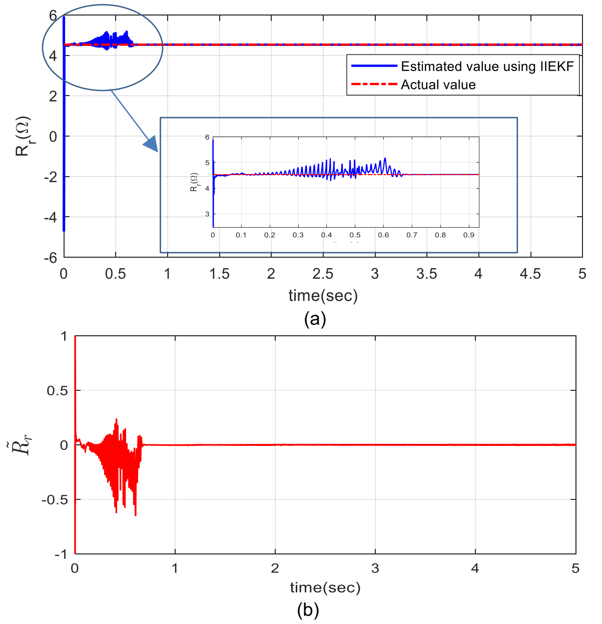

FIGURE 5. (a) Estimated of the rotor resistance and (b) Estimation error in nominal speed.

TABLE 3. Statistical characteristics of estimation errors.

Experiment number	Method	Variable	Root mean square	mean	Standard deviation
1	IIEKF	$\tilde{\omega}_r(k)$	1.6922	0.131	0.0132
		$\tilde{R}_r$	19.8806×10^{-3}	8.1180×10^{-4}	19.8803×10^{-3}
		$\tilde{R}_s$	8.2358×10^{-3}	3.0180×10^{-4}	8.1702×10^{-3}
2	IIEKF	$\tilde{\omega}_r(k)$	0.9800	0.3930	0.0310
		$\tilde{R}_r$	1.1782×10^{-3}	1.8486×10^{-6}	1.1781×10^{-3}
		$\tilde{R}_s$	10.5273×10^{-3}	1.2102×10^{-3}	10.4575×10^{-3}
	EKF	$\tilde{\omega}_r(k)$	4.99036	1.4486	0.1549
		$\tilde{R}_r$	2.1472×10^{-3}	1.8140×10^{-3}	1.1489×10^{-3}
		$\tilde{R}_s$	5.2364×10^{-3}	3.5069×10^{-3}	5.2364×10^{-3}

TABLE 4. Execution times for estimating the variables in 2nd experiment.

Method \ Estimated Variables	$(\omega_r(k), R_r)$	$(\omega_r(k), R_s)$
IIEKF	$25.9815(\mu\text{sec})$	$90.0867(\mu\text{sec})$
EKF	$24.4601(\mu\text{sec})$	$42.5746(\mu\text{sec})$

currents in the nominal speed in the *dq* stationary reference frame are shown in Figure 3.

According to section IV, the estimation process has been done. A computer with the following characteristics was used, CPU: Intel Core i7-7700HQ CPU @2.80GHz;16GB RAM. OS: Windows 10, 64. The results of the estimation of $\omega_r(k)$, R_r, and R_s using two experiments are presented as follows.

As described above, two experiments have been performed under a diverse range of operational loads and speeds. Then, the validation of the estimation process based on section IV, estimation of $\omega_r(k)$, R_r, and R_s, has been investigated for two ranges of speed as follows:

A. SCENARIO 1 $\omega_r(k) = [0 \sim 3000](RPM)$

The results of the estimation of $\omega_r(k)$, R_r, R_s and the estimation errors, $\tilde{\omega}_r(k)$, $\tilde{R}_r$, and $\tilde{R}_s$, for the 1st experiment are shown in Figures 4 to 6. In order to analyze the $\tilde{\omega}_r(k)$, $\tilde{R}_r$, and $\tilde{R}_s$, the root mean square errors and standard deviations of $\tilde{\omega}_r(k)$, $\tilde{R}_r$, and $\tilde{R}_s$ for the 1st experiment are shown in Table 3. Figures 4 to 6, and the related rows of 1st experiments in Table 3 show the whiteness of the estimation error, which indicate that the estimated parameters have acceptable accuracy.

B. SCENARIO 2 $\omega_r(k) = [0 \sim 1000](RPM)$

In this sub-section, in order to compare IIEKF and EKF, the estimation results of these two methods by using the dataset of 2nd experiment are shown in Figures 7 to 9. According to Figures 7 to 9, the estimation errors, $\tilde{\omega}_r(k)$, $\tilde{R}_r$ and $\tilde{R}_s$, using IIEKF are less than EKF.

In order to analyze the $\tilde{\omega}_r(k)$, $\tilde{R}_r$, and $\tilde{R}_s$, the root mean square errors and standard deviations of $\tilde{\omega}_r(k)$, $\tilde{R}_r$, and $\tilde{R}_s$ for the 2nd experiment are shown in Table 3. Similar to the 1st experiment, analyzing the estimation errors using IIEKF in Figures 7 to 9, and the related rows of the 2nd experiments in Table 3 (4th to 6th rows) show its whiteness and indicate that the estimated parameters have acceptable accuracy. By comparing the estimation errors using IIEKF with the estimation errors using EKF in Table 3 (4th to 9th rows), the estimation

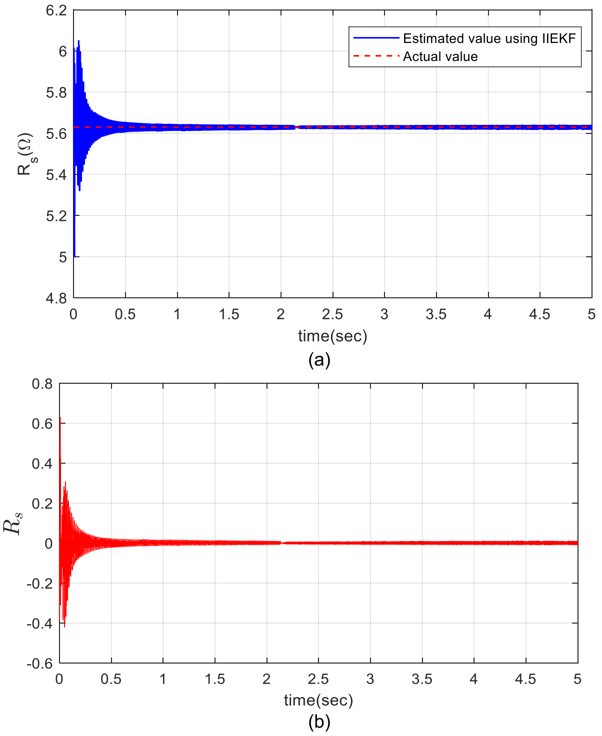

FIGURE 6. (a) Estimated of the stator resistance and (b) Estimation error in nominal speed.

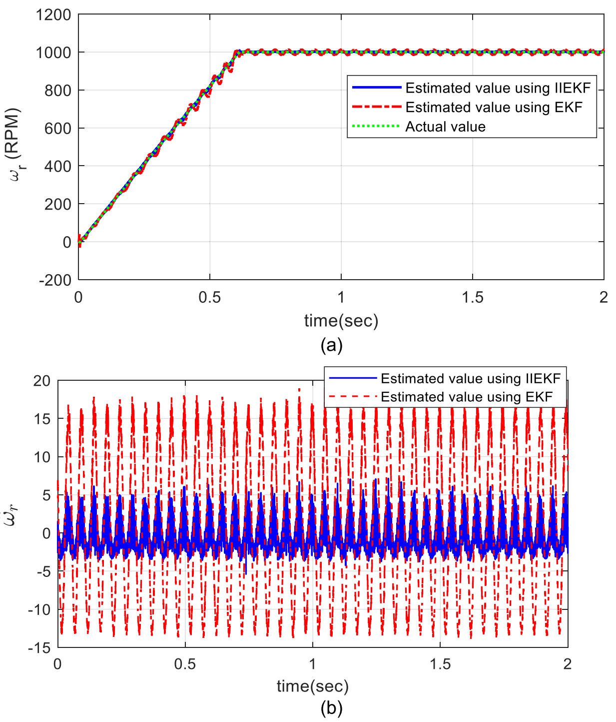

FIGURE 7. (a) Estimated of the rotor rotational speed and (b) Estimation error in low speed.

errors using IIEKF are less and closer to whiteness than the estimation errors using EKF.

Also, to compare the execution time of both methods, Table 4 is presented. According to Table 4, the execution time for running IIEKF is more than the execution times for running EKF. Obviously, more execution time in IIEKF

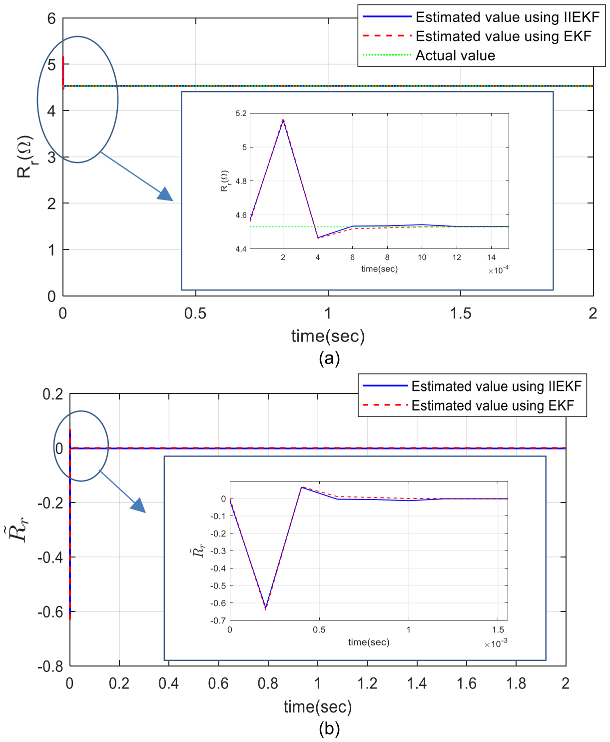

FIGURE 8. (a) Estimated of the rotor resistance and (b) Estimation error in low speed.

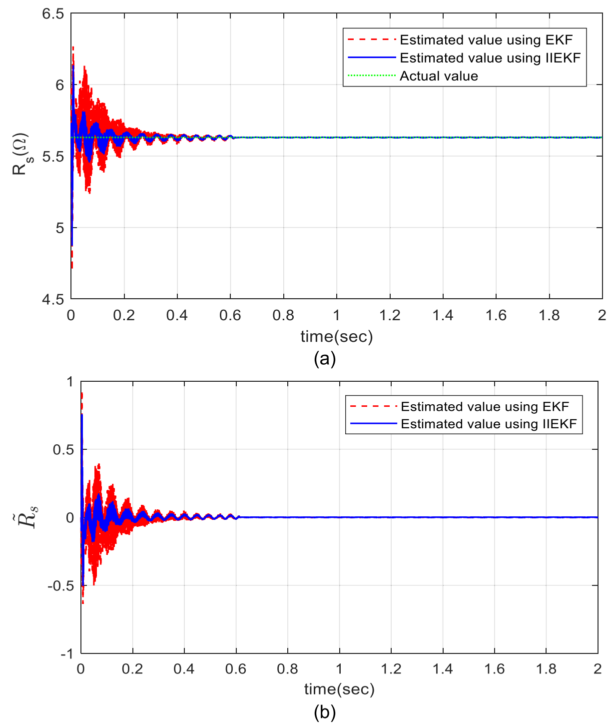

FIGURE 9. (a) Estimated of the stator resistance and (b) Estimation error in low speed.

because of the delay in obtaining the output signal owing to iterations have occurred. By considering execution times, IIEKF can be employed in the controllers where the execution times for estimating processes are less than the acceptable delay.

Therefore, according to Tables 3, 4, and Figures 4 to 9, the advantage of IIEKF in comparison with using EKF is its fewer estimation errors, and the disadvantage of IIEKF in comparison with using EKF is its execution estimation time.

According to the above results for both scenarios, the IIEKF works properly by using the extracted state-space models of the IM in (12) and (20) for estimating $\omega_r(k)$, R_r, and R_s.

VI. CONCLUSION

This paper introduced Improved Iterated Extended Kalman Filter (IIEKF) to estimate the rotational speed, stator, and rotor resistances. The performance of the IIEKF has been verified under real conditions and using experimental data. The results of estimation in the experimental results show that the applied method gives a reliable and accurate estimation for a three-phase IM under different operating conditions. Therefore, the effectiveness of the introduced approach has been shown.

Further research can be done by introducing a novel methodology to estimate rotational speed, rotor, and stator resistances in the presence of uncertainty and fault.

ACKNOWLEDGMENT

The authors would like to thank the Advanced Motor Control Laboratory, Iran University of Science and Technology (IUST), and also would like to thank Mahyar Khosravi, Ph.D, who attempted to provide all required experimental equipment.

REFERENCES

[1] D. Perdukova, P. Palacky, P. Fedor, P. Bober, and V. Fedak, ''Dynamic identification of rotor magnetic flux, torque and rotor resistance of induction motor,'' *IEEE Access*, vol. 8, pp. 142003–142015, 2020.

[2] H. A. Toliyat, S. Nandi, S. Choi, and H. Meshgin-Kelk, *Electric Machines: Modeling, Condition Monitoring, and Fault Diagnosis*. Boca Raton, FL, USA: CRC Press, 2012.

[3] N. El Ouanjli, A. Derouich, A. E. Ghzizal, S. Motahhir, A. Chebabhi, Y. E. Mourabit, and M. Taoussi, ''Modern improvement techniques of direct torque control for induction motor drives—A review,'' *Protection Control Modern Power Syst.*, vol. 4, no. 1, pp. 1–12, Dec. 2019.

[4] U. R. Muduli, R. K. Behera, K. Al Hosani, and M. S. E. Moursi, ''Direct torque control with constant switching frequency for three-to-five phase direct matrix converter fed five-phase induction motor drive,'' *IEEE Trans. Power Electron.*, vol. 37, no. 9, pp. 11019–11033, Sep. 2022.

[5] M. L. Jayaramu, H. N. Suresh, M. S. Bhaskar, D. Almakhles, S. Padmanaban, and U. Subramaniam, ''Real-time implementation of extended Kalman filter observer with improved speed estimation for sensorless control,'' *IEEE Access*, vol. 9, pp. 50452–50465, 2021.

[6] G.-J. Jo and J.-W. Choi, ''Rotor flux estimator design with offset extractor for sensorless-driven induction motors,'' *IEEE Trans. Power Electron.*, vol. 37, no. 4, pp. 4497–4510, Apr. 2022.

[7] L. A. Trujillo-Guajardo, J. Rodriguez-Maldonado, M. A. Moonem, and M. A. Platas-Garza, ''A multiresolution Taylor–Kalman approach for broken rotor bar detection in cage induction motors,'' *IEEE Trans. Instrum. Meas.*, vol. 67, no. 6, pp. 1317–1328, Jun. 2018.

[8] H. Abdallah and K. Benatman, ''Stator winding inter-turn short-circuit detection in induction motors by parameter identification,'' *IET Electric Power Appl.*, vol. 11, no. 2, pp. 272–288, Feb. 2017.

[9] T. Ameid, A. Menacer, H. Talhaoui, and I. Harzelli, ''Rotor resistance estimation using extended Kalman filter and spectral analysis for rotor bar fault diagnosis of sensorless vector control induction motor,'' *Measurement*, vol. 111, pp. 243–259, Dec. 2017.

[10] A. Menacer, S. Moreau, and G. Champenois, ''Parameters identification of the induction machine using a non linear parametric technique,'' *EPE J.*, vol. 22, no. 4, pp. 25–30, Dec. 2012.

[11] P. Cao, X. Zhang, and S. Yang, ''A unified-model-based analysis of MRAS for online rotor time constant estimation in an induction motor drive,'' *IEEE Trans. Ind. Electron.*, vol. 64, no. 6, pp. 4361–4371, Jun. 2017.

[12] J. J. Guedes, M. F. Castoldi, A. Goedtel, C. M. Agulhari, and D. S. Sanches, ''Parameters estimation of three-phase induction motors using differential evolution,'' *Electric Power Syst. Res.*, vol. 154, pp. 204–212, Jan. 2018.

[13] A. Lalami, R. Wamkeue, I. Kamwa, and M. Saad, ''Unscented Kalman filter for non-linear estimation of induction machine parameters,'' *IET Electr. Power Appl.*, vol. 6, no. 9, pp. 611–620, Nov. 2012.

[14] A. A. Tanvir and A. Merabet, ''Artificial neural network and Kalman filter for estimation and control in standalone induction generator wind energy DC microgrid,'' *Energies*, vol. 13, no. 7, p. 1743, Apr. 2020.

[15] Y. Zhang, X. Wang, H. Yang, B. Zhang, and J. Rodriguez, ''Robust predictive current control of induction motors based on linear extended state observer,'' *Chin. J. Electr. Eng.*, vol. 7, no. 1, pp. 94–105, Apr. 2021.

[16] N. Pimkumwong and M.-S. Wang, ''Online speed estimation using artificial neural network for speed sensorless direct torque control of induction motor based on constant V/F control technique,'' *Energies*, vol. 11, no. 8, p. 2176, Aug. 2018.

[17] M. Korzonek, G. Tarchala, and T. Orlowska-Kowalska, ''A review on MRAS-type speed estimators for reliable and efficient induction motor drives,'' *ISA Trans.*, vol. 93, pp. 1–13, Oct. 2019.

[18] C. Lascu, I. Boldea, and F. Blaabjerg, ''Comparative study of adaptive and inherently sensorless observers for variable-speed induction-motor drives,'' *IEEE Trans. Ind. Electron.*, vol. 53, no. 1, pp. 57–65, Feb. 2006.

[19] S. Kumar, J. Prakash, and P. Kanagasabapathy, ''A critical evaluation and experimental verification of extended Kalman filter, unscented Kalman filter and neural state filter for state estimation of three phase induction motor,'' *Appl. Soft Comput.*, vol. 11, no. 3, pp. 3199–3208, Apr. 2011.

[20] M. Farza, M. M'Saad, T. Ménard, A. Ltaief, and T. Maatoug, ''Adaptive observer design for a class of nonlinear systems. Application to speed sensorless induction motor,'' *Automatica*, vol. 90, pp. 239–247, Apr. 2018.

[21] H. Wang, Y.-C. Liu, and X. Ge, ''Sliding-mode observer-based speed-sensorless vector control of linear induction motor with a parallel secondary resistance online identification,'' *IET Electr. Power Appl.*, vol. 12, no. 8, pp. 1215–1224, Sep. 2018.

[22] M. S. Zaky, M. K. Metwaly, H. Z. Azazi, and S. A. Deraz, ''A new adaptive smo for speed estimation of sensorless induction motor drives at zero and very low frequencies,'' *IEEE Trans. Ind. Electron.*, vol. 65, no. 9, pp. 6901–6911, Sep. 2018.

[23] E. Zerdali, ''A comparative study on adaptive EKF observers for state and parameter estimation of induction motor,'' *IEEE Trans. Energy Convers.*, vol. 35, no. 3, pp. 1443–1452, Sep. 2020.

[24] Z. Masoumi, B. Moaveni, M. Khorshidi, J. Faiz, and S. M. M. Gazafrudi, ''Experimental parameter estimation of induction motor based on transient and steady-state responses in synchronous and rotor reference frames,'' *IEEE Trans. Energy Convers.*, vol. 37, no. 1, pp. 145–152, Mar. 2022.

[25] R. Yildiz, M. Barut, and R. Demir, ''Extended Kalman filter based estimations for improving speed-sensored control performance of induction motors,'' *IET Electric Power Appl.*, vol. 14, no. 12, pp. 2471–2479, Dec. 2020.

[26] G. Ozkurt and E. Zerdali, ''Design and implementation of hybrid adaptive extended Kalman filter for state estimation of induction motor,'' *IEEE Trans. Instrum. Meas.*, vol. 71, pp. 1–12, 2022.

[27] K.-H. Kim, G.-I. Jee, C.-G. Park, and J.-G. Lee, ''The stability analysis of the adaptive fading extended Kalman filter using the innovation covariance,'' *Int. J. Control Autom. Syst.*, vol. 7, no. 1, pp. 49–56, 2009.

[28] C.-M. Lee and C.-L. Chen, ''Observer-based speed estimation method for sensorless vector control of induction motors,'' *IEE Proc. Control Theory Appl.*, vol. 145, no. 3, pp. 359–363, May 1998.

[29] K. L. Shi, T. F. Chan, Y. K. Wong, and S. L. Ho, ''Speed estimation of an induction motor drive using an optimized extended Kalman filter,'' *IEEE Trans. Ind. Electron.*, vol. 49, no. 1, pp. 124–133, Feb. 2002.

[30] E. Zerdali and M. Barut, "The comparisons of optimized extended Kalman filters for speed-sensorless control of induction motors," *IEEE Trans. Ind. Electron.*, vol. 64, no. 6, pp. 4340–4351, Jun. 2017.

[31] M. Barut, S. Bogosyan, and M. Gokasan, "Experimental evaluation of braided EKF for sensorless control of induction motors," *IEEE Trans. Ind. Electron.*, vol. 55, no. 2, pp. 620–632, Feb. 2008.

[32] E. Zerdali, "Adaptive extended Kalman filter for speed-sensorless control of induction motors," *IEEE Trans. Energy Convers.*, vol. 34, no. 2, pp. 789–800, Jun. 2018.

[33] L. Tian, Z. Li, Z. Wang, X. Sun, T. Guo, and H. Zhang, "Speed-sensorless control of induction motors based on adaptive EKF," *J. Power Electron.*, vol. 21, no. 12, pp. 1823–1833, Dec. 2021.

[34] B. Akin, U. Orguner, A. Ersak, and M. Ehsani, "A comparative study on non-linear state estimators applied to sensorless AC drives: MRAS and Kalman filter," in *Proc. 30th Annu. Conf. IEEE Ind. Electron. Soc. (IECON)*, Nov. 2004, pp. 2148–2153.

[35] Y.-R. Kim, S.-K. Sul, and M.-H. Park, "Speed sensorless vector control of induction motor using extended Kalman filter," *IEEE Trans. Ind. Appl.*, vol. 30, no. 5, pp. 1225–1233, Sep. 1994.

[36] Y. Wenqiang, J. Zhengchun, and X. Qiang, "A new algorithm for flux and speed estimation in induction machine," in *Proc. 5th Int. Conf. Electr. Mach. Syst. (ICEMS)*, 2001, pp. 698–701.

[37] Q. Ge and Z. Feng, "Speed estimated for vector control of induction motor using reduced-order extended Kalman filter," in *Proc. 3rd Int. Power Electron. Motion Control Conf. (IPEMC)*, 2000, pp. 138–142.

[38] M. Barut, R. Demir, E. Zerdali, and R. Inan, "Real-time implementation of bi input-extended Kalman filter-based estimator for speed-sensorless control of induction motors," *IEEE Trans. Ind. Electron.*, vol. 59, no. 11, pp. 4197–4206, Dec. 2011.

[39] C. El Moucary, G. Garcia Soto, and E. Mendes, "Robust rotor flux, rotor resistance and speed estimation of an induction machine using the extended Kalman filter," in *Proc. IEEE Int. Symp. Ind. Electron. (ISIE)*, Jul. 1999, pp. 742–746.

[40] M. Barut, S. Bogosyan, and M. Gokasan, "Speed sensorless direct torque control of IMs with rotor resistance estimation," *Energy Convers. Manage.*, vol. 46, no. 3, pp. 335–349, Feb. 2005.

[41] J. Faiz and M. B. B. Sharifian, "Different techniques for real time estimation of an induction motor rotor resistance in sensorless direct torque control for electric vehicle," *IEEE Trans. Energy Convers.*, vol. 16, no. 1, pp. 104–109, Mar. 2001.

[42] A. Taheri, H.-P. Ren, and C.-H. Song, "Sensorless direct torque control of the six-phase induction motor by fast reduced order extended Kalman filter," *Complexity*, vol. 2020, pp. 1–10, Sep. 2020.

[43] B. Akin, U. Orguner, A. Ersak, and M. Ehsani, "Simple derivative-free nonlinear state observer for sensorless AC drives," *IEEE/ASME Trans. Mechatronics*, vol. 11, no. 5, pp. 634–643, Oct. 2006.

[44] R. Yildiz, M. Barut, and E. Zerdali, "A comprehensive comparison of extended and unscented Kalman filters for speed-sensorless control applications of induction motors," *IEEE Trans. Ind. Informat.*, vol. 16, no. 10, pp. 6423–6432, Oct. 2020.

[45] M. S. Zaky, M. M. Khater, S. S. Shokralla, and H. A. Yasin, "Wide-speed-range estimation with online parameter identification schemes of sensorless induction motor drives," *IEEE Trans. Ind. Electron.*, vol. 56, no. 5, pp. 1699–1707, May 2008.

[46] S. Haykin, *Kalman Filtering and Neural Networks*, vol. 284. Hoboken, NJ, USA: Wiley, 2001.

[47] L. Fan and Y. Wehbe, "Extended Kalman filtering based real-time dynamic state and parameter estimation using PMU data," *Electr. Power Syst. Res.*, vol. 103, pp. 168–177, Oct. 2013.

[48] N. Zhou, D. Meng, Z. Huang, and G. Welch, "Dynamic state estimation of a synchronous machine using PMU data: A comparative study," *IEEE Trans. Smart Grid*, vol. 6, no. 1, pp. 450–460, Jan. 2014.

[49] J. Zhao, M. Netto, and L. Mili, "A robust iterated extended Kalman filter for power system dynamic state estimation," *IEEE Trans. Power Syst.*, vol. 32, no. 4, pp. 3205–3216, Jul. 2016.

[50] S. Gao, Y. Zhong, X. Zhang, and B. Shirinzadeh, "Multi-sensor optimal data fusion for INS/GPS/SAR integrated navigation system," *Aerosp. Sci. Technol.*, vol. 13, nos. 4–5, pp. 232–237, Jun. 2009.

BIJAN MOAVENI received the B.Sc. degree in control engineering from the Isfahan University of Technology, Isfahan, Iran, in 2000, and the M.Sc. and Ph.D. degrees in control engineering from the K. N. Toosi University of Technology, Tehran, Iran, in 2002 and 2007, respectively.

From 2009 to 2015, he was an Assistant Professor, and from 2015 to 2018, he was an Associate Professor with the Department of Control and Signaling, School of Railway Engineering, Iran University of Science and Technology, Tehran. Since 2018, he has been an Associate Professor with the Systems and Control Engineering Group, K. N. Toosi University of Technology. He is also a member of the Center of Excellence for Modelling and Control of Complex Systems. He has authored or coauthored two books and more than 100 articles. His current research interests include large-scale control systems, control configuration selection, robust control systems, estimation theory, and automatic traffic control systems.

ZAHRA MASOUMI received the B.Sc. degree in electronic engineering from QIAU, Qazvin, Iran, in 2013, and the M.Sc. and Ph.D. degrees in control and signaling engineering from the Control and Signaling Department, School of Railway Engineering, Iran University of Science and Technology, Tehran, Iran, in 2017 and 2022, respectively.

PEGAH RAHMANI was born in Qazvin, Iran, in August 1990. She received the B.Sc. degree in electrical engineering from Zanjan University, in 2014, and the M.Sc. degree in control and signaling engineering from the Iran University of Science and Technology, in 2020.

Since 2021, she has been working in turbo machinery as an Electrical and Instrumentation Engineer. Simultaneously, she has conducted research on electric vehicles (Evs), mostly on battery management systems (BMS), and she has been writing a review paper on it and preparing herself for the Ph.D. study.